

# Measuring Extracellular Ion Gradients from Single Channels with Ion-Selective Microelectrodes

Mark A. Messerli, Erica D. Corson, and Peter J. S. Smith

BioCurrents Research Center, Program in Molecular Physiology, Marine Biological Laboratory, Woods Hole, Massachusetts

**ABSTRACT** Under many different conditions activated plasma membrane ion channels give rise to changes in the extracellular concentration of the permeant ion(s). The magnitude and duration of these changes are dependent on the electrochemical driving force(s) on the permeant ion(s) as well as conductance, open time, and channel density. We have modeled the change in the extracellular  $[K^+]$  due to efflux through  $Ca^{2+}$ -activated  $K^+$  channels, mSlo, to determine the range of parameters that would give rise to measurable signals in the surrounding media. Subsequently we have used extracellular,  $K^+$ -selective microelectrodes to monitor localized changes in  $[K^+]_{ext}$  due to efflux through mSlo channels expressed in *Xenopus* oocytes. The rapid changes in  $[K^+]$  show a close fit with the predicted model when the time response of the ion-selective microelectrode is taken into account, providing proof of the concept. Measurement of the change in extracellular ion concentration with ion-selective microelectrodes provides a noninvasive means for functional mapping of channel location and density, as well as characterizing the properties of ion channels in the plasma membrane.

Received for publication 12 December 2006 and in final form 16 January 2007.

Address reprint requests and inquiries to Peter J. S. Smith, Fax: 508-540-6902; E-mail: psmith@mbl.edu.

Ion-selective microelectrodes (ISMs) have been used to measure steady and dynamic changes in extracellular ion concentration at the surface of single cells and tissues (1,2). In many cases the combined activity of a population of a single type of channel or transporter leads to the majority of the extracellular ion concentration change for a specific ion. In theory, ISMs possess the sensitivity and time response for measuring localized changes in ion concentration due to flux through a single ion channel. We have used a combination of extracellular ion gradient modeling, measurement, and fitting to prove the feasibility and explore the applicability of this hypothesis.

$[K^+]$  changes at the external side of the  $Ca^{2+}$ -activated  $K^+$  channel, mSlo, were calculated assuming diffusion from a point source. The equation below describes diffusion into a hemisphere due to restricted diffusion imposed by the plasma membrane

$$C(r, t) = \frac{2m}{(4\pi Dt)^{3/2}} e^{-r^2/4Dt},$$

where the concentration ( $C$ ) varies over a radial distance ( $r$ ) with time ( $t$ ) and is dependent on the total mols ( $m$ ) passed through the channel and the diffusion coefficient ( $D$ ) of the ion ( $D_{K^+} = 1.96 \times 10^{-5} \text{ cm}^2/\text{s}$ ). The equation provides the concentration profile at a point in time after instantaneous release from a point source. The concentration profile near the ion channel was modeled by assuming that the concentration at any point from the channel is the sum of all the instantaneous releases during the open time of the channel, with instantaneous release being the amount of ions that passed through the channel in 0.1 ms. This time step generated a concentration profile that was, on average, within 0.01% of the values generated with a shorter time step of 0.01ms. The  $[K^+]_{ext}$  was converted to a predicted

measured voltage by the  $K^+$ -selective ISM using the Nernst equation and background  $[K^+]$  in the bath. The time response of the ISM ( $t_{95\%}$ ) was modeled as three time constants of an RC circuit.

Activation of the mSlo channel at membrane potentials more positive than the  $K^+$  equilibrium potential ( $K_{eq}^+$ ) will give rise to  $K^+$  efflux. Modeling was therefore constrained to the resulting increase in  $[K^+]$  at the extracellular side of the channel. This increase is dependent on channel conductance to the permeant ion(s), the electrochemical driving force(s) on the permeant ion(s), channel open time, and distance from the channel. Single-channel conductance of 272 pS was determined during initial characterization of mSlo in *Xenopus* oocytes (3).

Fig. 1, A–C, shows the change in  $[K^+]$  that occurs for ranges of the three remaining parameters. A modified form of the Goldman-Hodgkin-Katz equation was used to determine the number of  $K^+$  ions that would leave the cell through the channel under different depolarizing potentials. The  $K_{eq}^+$  in *Xenopus* oocytes is  $\sim -88$  mV under normal conditions. The peak change in  $[K^+]$  2  $\mu\text{m}$  from the channel is only 0.06  $\mu\text{M}$  when the membrane potential is driven to  $-80$  mV. Depolarizing the membrane potential further away from the  $K_{eq}^+$   $-40$ ,  $0$ ,  $+40$ , and  $+80$  mV leads to an average  $[K^+]$  increase of 0.9, 2.4, 4.9, and 8.1  $\mu\text{M}$ , respectively, for a channel with an open time of 100 ms. The profile of the  $[K^+]$  changes as a function of open time, appearing as a spike for channel events shorter than 30 ms but reaching a relative steady-state plateau for events longer than 100 ms, as shown

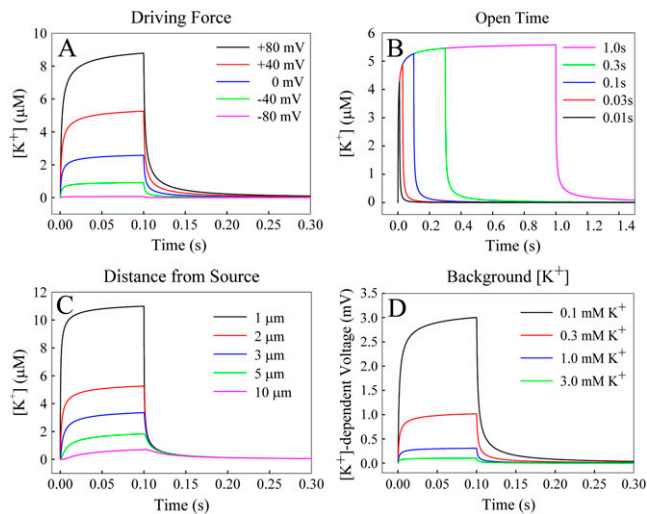


**FIGURE 1** Models of  $[K^+]_{\text{ext}}$  changes near an activated mSlo channel with varying driving force on  $K^+$  (A) open time (B) distance from the channel (C) and when measured with an ideal  $K^+$  ISM in varying background  $[K^+]$  (D).

in Fig. 1 B. These profiles were generated for a  $[K^+]$  at  $2 \mu\text{M}$  from the channel with a  $+40 \text{ mV}$  membrane potential. Under these conditions the  $[K^+]_{\text{ext}}$  rises  $>4 \mu\text{M}$  for even a brief 10-ms event. Diffusion of  $K^+$  away from the channel leads to dilution of the  $[K^+]$  as displayed in Fig. 1 C. The voltage response of the detecting ISM is dependent on the background  $[K^+]$ . Larger voltages will occur for the same rise in  $[K^+]$  with lower background  $[K^+]$  as displayed in Fig. 1 D. In normal OR-2,  $3 \text{ mM } K^+$ , the voltage response will peak at  $<0.1 \text{ mV}$ , at  $2 \mu\text{m}$  from the channel with  $+40 \text{ mV}$  membrane potential. However, the voltage response of the ISM increases 10- to 30-fold for a proportional decrease in background  $[K^+]$ . Modeling in Fig. 1 D assumes an ISM with an instantaneous response. In a flow exchange system, a  $K^+$  ISM measured a  $193 \pm 4 \mu\text{V}$  difference for a  $[K^+]$  change from 100 to 101  $\mu\text{M}$ . Peak-to-peak noise was  $45 \mu\text{V}$ .

Measurements of single-channel events were performed on *Xenopus* oocytes expressing the mSlo channel. Oocytes were injected with 50 nL of increasing dilutions of mSlo RNA to obtain low channel density,  $\sim 1$  channel per  $50 \mu\text{m}^2$ , thereby increasing the probability of capturing isolated channel events. Recordings were collected from oocytes in  $0.1 \text{ mM } K^+$  OR-2. The coelomic envelope was left intact during recordings to maintain the integrity of the plasma membrane and provide structural support.

$K^+$  ISMs were used to measure the increase in  $[K^+]_{\text{ext}}$  next to the surface of the plasma membrane of oocytes overexpressing the mSlo channel and water-injected controls. The mSlo channels are activated by cytosolic  $\text{Ca}^{2+}$  and depolarization; higher cytosolic  $\text{Ca}^{2+}$  leads to channel activation at less positive potentials (3). Due to enhanced difficulty with reliably controlling the cytosolic  $[\text{Ca}^{2+}]$ , we activated the channels under resting cytosolic  $[\text{Ca}^{2+}]$  with more positive depolarizing

potentials. Voltage and current passing electrodes impaled the oocyte at the equator whereas the  $K^+$  ISM was placed near the animal pole. The ISM was advanced far enough to induce dimpling of the coelomic envelope and then was backed up until the coelomic envelope was no longer dimpled. Depolarization of the plasma membrane caused a large brief electrical transient followed by a slow increase in the  $[K^+]$ -dependent voltage recorded by the ISM next to water-injected controls as well as mSlo RNA-injected oocytes. Fig. 2 A shows the large increase in the  $[K^+]$ -dependent voltage recorded by an ISM next to an oocyte overexpressing mSlo and depolarized to  $+40 \text{ mV}$ . The background  $[K^+]$  recovered over a similar time course upon repolarization to resting membrane potential. This large increase in  $[K^+]_{\text{ext}}$  upon depolarization is likely due to  $K^+$  efflux through the five different types of endogenous  $K^+$  channels normally expressed in *Xenopus* oocytes and activated at this potential (4).  $K^+$  efflux through endogenous channels raised the local background  $[K^+]$  from 0.1 to  $>0.3 \text{ mM}$ . Despite the threefold increase in background  $[K^+]$ , upon depolarization, relatively rapid transient changes in  $[K^+]$  were still detected only in depolarized mSlo expressing oocytes. The larger events are underlined in Fig. 2. The first cluster of events in Fig. 2 is magnified in the inset. No such transients were measured on the  $[K^+]$ -dependent voltage acquired during repolarization of mSlo expressing oocytes or in control oocytes. The transients are not due to current-generated voltages that peak at only  $2.3 \mu\text{V}$ ,  $1 \mu\text{m}$  from the channel, under these conditions. In support of this statement, a current-passing  $K^+$ -selective ISM was used to generate local, transient  $[K^+]$  increases. Near the source a second  $K^+$  ISM measured 1–1.5 mV  $[K^+]$ -dependent voltage increases, but no corresponding voltage changes were measured with open barreled electrodes.

The large conductance mSlo channels produce a signal that is separable from the lower conductance endogenous  $K^+$

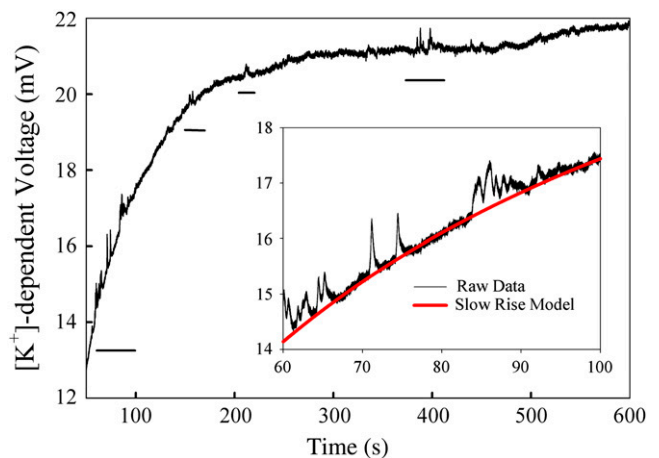


**FIGURE 2** Raw voltage output of a  $K^+$ -selective microelectrode near a depolarized *Xenopus* oocyte expressing the mSlo channel. The inset shows amplification of the 60- to 100-s region with an overlay of the model for the slow rise in  $[K^+]$  (red).

channels. To perform a direct comparison of the measured mSlo activity to the modeled mSlo channels we removed the large basal increase in  $[K^+]_{ext}$ . A seven-parameter exponential fit model, was used to find a close match to the large slow increase in  $[K^+]_{ext}$ . Three single-channel events were isolated for further analysis by subtracting the modeled slow rise from the raw recording and are shown in Fig. 3, A–C. Events 1 and 2 are isolated from other mSlo events whereas event 3 is sandwiched between two other events. A best-fit alignment between the model and the measured  $[K^+]_{ext}$ -dependent voltage output of the ISM was performed by varying ion channel model parameters and ISM response times and minimizing the sum of the squares of the differences between the two as they were shifted in time with respect to each other. A 2-s duration profile was used for each of the three modeled events. Distance of the ISM from the ion channel was incremented by  $0.01 \mu\text{m}$ , whereas the channel open time and ISM response time were incremented by 1 and 5 ms, respectively. The black profile shows the  $[K^+]_{ext}$ -dependent voltage measured by the ISM whereas the overlaid red profile shows a best-fit alignment of the model. The ISM was modeled with varying response times to perform the best-fit alignment because the actual response time of the electrode was not determined during recordings. Table 1 shows the best-fit parameters for each event.

According to these parameters, channel events 1 and 2 are slightly  $>1 \mu\text{m}$  from the ISM whereas channel event 3 is  $2.3 \mu\text{m}$  away. The diffusion profile contains information regarding the absolute distance from the ISM but not the vector position of the channel from the ISM. Future work with three closely positioned ISMs could be used to determine the exact position of the channel with respect to the ISMs.

The relatively slow response time of the measuring system is the weakest aspect of this detection method. As a result, shorter duration and lower conductance channel events were missed during these recordings. Also, the signals shown in Fig. 3, A–C, are attenuated. Assuming an instantaneous ISM response time, the profiles for the three events would be much

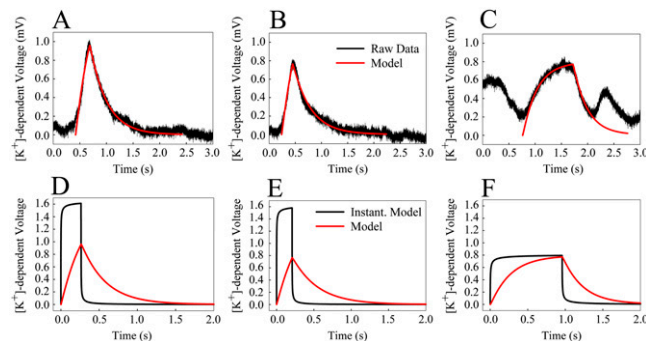


**FIGURE 3 (A–C) Raw recordings (black) with overlaid best-fit models (red) of increased  $[K^+]_{ext}$  from single mSlo channels. (D–F) Best-fit models (red) and instantaneous electrode response time models (black) of single-channel events from panels A–C.**

**TABLE 1 Best-fit modeled parameters from measured single-channel events**

Modeled parameter	Event 1	Event 2	Event 3
Background $[K^+]_{ext}$	349 $\mu\text{M}$	353 $\mu\text{M}$	366 $\mu\text{M}$
Distance from ISM	1.11 $\mu\text{m}$	1.13 $\mu\text{m}$	2.27 $\mu\text{m}$
Open time	264 ms	208 ms	958 ms
ISM time constant	305 ms	325 ms	250 ms

easier to distinguish as shown in Fig. 3, D–F. Although ISMs with instantaneous responses are only theoretically possible, ISMs with response times between 5 and 25 ms have been reported (5,6) and will be critical for accurately monitoring signals from channels with smaller conductance and shorter open time. If response time can be improved to this level then ion gradients from single channels with 50 and 20 pS conductance will produce  $[K^+]_{ext}$ -dependent voltages above 320 and 125  $\mu\text{V}$ , respectively, after 20 ms open time at  $1 \mu\text{m}$  from the cell with a  $+40 \text{ mV}$  membrane potential. Our emphasis here has been on the modeling and detection of single channels. However, in practice, ion channel densities range from  $<1$  to  $>10,000 \mu\text{m}^{-2}$  (7), indicating that substantially larger ion gradients will be established and more complex signal extraction methods will be needed to functionally map and characterize channels with extracellular ISMs.

## ACKNOWLEDGMENTS

The mSlo channel sequence was kindly provided by Dr. L. Kaczmarek (Yale University, New Haven, CT).

This research was funded by National Institutes of Health-National Center for Research Resources grant No. P41 RR001395 to P.J.S.S.

## REFERENCES and FOOTNOTES

- Messerli, M. A., K. R. Robinson, and P. J. S. Smith. 2006. Electrochemical sensor applications to the study of molecular physiology and analyte flux in plants. *In Plant Electrophysiology Theory and Methods*. A. G. Volkov, editor. Springer-Verlag, Berlin and Heidelberg, Germany. 73–104.
- Smith, P. J. S., R. H. Sanger, and M. A. Messerli. 2007. Principles, development and applications of self-referencing electrochemical microelectrodes to the determination of fluxes at cell membranes. *In Electrochemical Methods for Neuroscience*. A. C. Michael and L. M. Borland, editors. CRC Press, Boca Raton, FL. 373–405.
- Butler, A., S. Tsunoda, D. P. McCobb, A. Wei, and L. Salkoff. 1993. mSlo, a complex mouse gene encoding “maxi” calcium-activated potassium channels. *Science*. 261:221–224.
- Weber, W.-M. 1999. Endogenous ion channels in oocytes of *Xenopus laevis*: recent developments. *J. Membr. Biol.* 170:1–12.
- Ujec, E., E. E. O. Keller, N. Křiž, V. Pavlík, and J. Machek. 1980. Low-impedance, coaxial, ion-selective, double-barrel microelectrodes and their use in biological measurements. *J. Electroanal. Chem.* 116:363–369.
- Pumain, R., I. Kurcewicz, and J. Louvel. 1983. Fast extracellular calcium transients: involvement in epileptic processes. *Science*. 222: 177–179.
- Hille, B. 2001 *Ion Channels of Excitable Membranes*. Sinauer Associates, Sunderland, MA.